

Understanding the hydrochemical evolution of a coastal dune system in SW England using a multiple tracer technique

Debbie Allen¹, W George Darling¹, Peter J Williams¹, Charlie J Stratford², Nick S Robins¹

¹British Geological Survey, Maclean Building, Wallingford, OX10 8BB, UK.

²Centre of Ecology and Hydrology, Maclean Building, Wallingford, OX10 8BB, UK.

Corresponding author: email dall@bgs.ac.uk, Tel 01491 692391, Fax 01491 692345

1 **Abstract** An improved knowledge of the hydrology of coastal dune systems is desirable for
2 successful management of their diverse ecology under a changing climate. As a near-pristine
3 coastal dune spit system, Braunton Burrows (SW England) is an ideal location for the study
4 of the natural processes governing recharge to the dune groundwater system and the
5 evolution of its water quality. Whereas previous investigations have tended to focus on inter-
6 dune slacks, this study has also given attention to infiltration through the high dunes. Cores
7 were taken through dunes and the resulting sand samples processed to provide information on
8 grain size distribution and porewater chemistry. Groundwater samples were obtained from
9 beneath dunes and slacks. A variety of geochemical techniques were applied including
10 hydrochemistry, stable isotopes and residence time indicators. The unsaturated zone profiles
11 indicate the existence of piston flow recharge with an infiltration rate of 0.75–1 m/yr,
12 although faster rates probably also occur locally. Groundwater beneath the high dunes gave
13 ages in the range 13–16 yr, compared to the dune slack groundwater ages of 5–7 yr, and an
14 age of 22 yr for groundwater from the underlying mudstone aquifer. The chemistry of waters
15 in both unsaturated and saturated zones is dominated by Ca and HCO₃, supplemented by
16 variable amounts of other ions derived from marine aerosols and limited reaction with sand
17 grains and their coatings. The main chemical evolution of the porewaters occurs rapidly
18 through the mobilisation of surface salt crusts and dissolution of shell carbonate. This
19 situation changes little in the underlying groundwater, though an evolution towards reducing
20 conditions increases the concentrations of redox-sensitive species such as Fe and Mn. The
21 rapid chemical evolution of the infiltrating water means that its composition will respond
22 quickly to changes in the supply of shell material and/or marine salts, which are possible
23 consequences of climate change. However, the residence time measurements suggest the
24 dune aquifer has a relatively long turnover time which will to some extent buffer such
25 changes. The results of the present study should be transferable to natural dune systems in
26 similar coastal situations.

27 Key words: dune, dune slack, wetland, hydrochemistry, stable isotopes, SF₆, unsaturated
28 zone, groundwater.

29 **1 INTRODUCTION**

30

31 Within Europe, coastal dune systems are widely distributed along the Atlantic,
32 Mediterranean, North Sea and Baltic littorals (Doody 2008). They include areas of open
33 mobile sand and more mature vegetated and relatively static dunes. The elevation of the
34 water table within the dunes partially dictates the morphology of the dune fields and
35 determines the elevation at which wetland dune slacks, the flat-floored depressions that occur
36 within the sand dunes, are formed (Stuyfzand 1993; Stratford et al. 2013). The slacks have a
37 shallow water table in summer and may be flooded for much of the winter. The hydrological
38 regime, coupled with the chemistry of the water, dictates the ecological status of the slacks
39 which tend towards a rich and diverse assemblage including rare species (Grootjans et al.
40 1998; Curreli et al. 2013).

41

42 A conceptual understanding of the processes controlling the hydrological regime in dune
43 systems is fundamental to conservation management. As the water table and water chemistry
44 determine the abundance of many slack species and control the vegetation assemblages
45 (Willis et al. 1959) knowledge of the hydrochemical processes and their stability is key to
46 informing management strategies to protect the slack ecosystems. Key questions are:

47

- 48 1. Does infiltration reach the water table exclusively by piston flow?
- 49 2. How does water quality evolve in the unsaturated and saturated zones beneath the
50 high dunes?
- 51 3. What kind of timescales are involved in the water movement and evolution?
- 52 4. Is water quality stable with time or could it change?

53

54 Conservation management also has to cope with coastal erosion and accretion which impact
55 groundwater base levels, changes in rainfall and other natural and sometimes catastrophic
56 events (Robins et al. 2013).

57

58 While there have been a number of studies of dune hydrology based on physical parameters
59 such as water levels (e.g. Van der Hagen et al 2008, Vandenbohede et al 2008, Clarke et al.
60 2010, Davy et al. 2010), there are fewer examples of dune water quality being applied to a
61 better understanding of hydrology and ecology (Stuyfzand 1993; Grootjans et al. 1996; Sival
62 et al. 1999). These studies either tended to focus on dune slacks or, particularly in the case of

63 pioneering work on dune system geochemistry (Stuyfzand 1993, Stuyfzand 1989), on
64 systems impacted by processes such as artificial recharge, salinization, decalcification and
65 anthropogenic drainage works. In contrast, this paper describes a study of the
66 hydrogeochemistry of a more natural dune groundwater system at Branton Burrows in North
67 Devon, England, based on data gathered from unsaturated zone profiles and piezometers
68 beneath both dune ridges and slacks. The techniques used include hydrochemistry, stable
69 isotopes and trace gas age indicators.

70

71 Investigations at Branton Burrows, as at many other coastal dune wetlands, have
72 concentrated mainly on understanding the ecohydrology of the dune slacks with less attention
73 being given to the high dunes. This reflects the importance of the slack ecosystems and their
74 conservation management compared to the sparsely-vegetated high dunes (Davy et al. 2006;
75 2010). However, understanding the hydrology of dune systems requires knowledge of
76 processes operating across the whole site rather than just the more ecologically complex
77 zones. The present study, therefore, focuses on both the hydrogeochemical processes beneath
78 the dune slacks and the high dunes. The objective is to provide supporting evidence for the
79 understanding of dune spit hydrology in order to better inform the needs for conservation
80 management.

81

82

83 **2 BACKGROUND**

84

85 Branton Burrows is a dune spit wetland on the North Devon coast in south-west England
86 (Fig. 1), rising in elevation to 38 m above Ordnance Datum (aOD) with an area some 10 km²
87 (Stratford et al. 2013). The spit comprises a series of N–S oriented dunes and slacks which
88 evolved in response to the dynamics of the prevailing wind and sea (Saye and Pye 2007). A
89 narrow zone of low fore-dunes, up to 5 m high, adjacent to the beach is succeeded inland by
90 sand hills up to 15 m high separated by a discontinuous belt of slacks. The highest dunes
91 occur just inland from these slacks beyond which is a broad, but poorly defined, belt of
92 lower-lying ground with scattered hillocks and many ephemeral and some permanent pools.
93 Further inland are lesser dunes followed by flat sands with a few scattered small dunes which
94 merge towards cultivated fields. The slacks mainly remain dry in winter with ephemeral wet
95 weather pools (Davy et al. 2006; 2010).

96

97 The dunes rest on an estuarine clay layer forming the base of the small rain-fed aquifer in the
98 sand (Burden 1998). The underlying Pilton Mudstone Formation (Devonian) forms a low-
99 yielding aquifer, with little to no hydraulic contact between this and the sand aquifer.
100 Groundwater level data from the piezometer network has been used to identify a groundwater
101 divide within the sands parallel to the beach some two-thirds of the way inland towards the
102 rear of the dune-field (Fig. 2). Groundwater discharges both to the beach beneath the fore-
103 dune and inland to estuarine deposits which form low-lying meadows. The water table
104 reaches a maximum elevation of 8 m aOD in winter along the axis of the groundwater divide
105 (Stratford et al. 2013). There has been a decline in rainfall over the last 40 years which has
106 caused a reduction in water table elevation which in turn has degraded the slack ecosystems
107 (Robins and Jones 2013). Comparison with other west coast dune sites in England and Wales
108 indicates that Braunton Burrows has been most impacted by change due to the decline in
109 effective rainfall, making a better understanding of its hydrology a priority.

110

111

112 **3 SAMPLING AND ANALYSIS**

113

114 Three new uncored shallow dipwells (BB1, BB2 and BB3, see Table 1, Fig. 1) were hand-
115 augered into the dune slacks to supplement an existing groundwater level monitoring network
116 and to provide access for groundwater sampling. Subsequently a trial ‘deep’ cored dipwell
117 (D1) was hammer drilled to a depth ~6 m on a high dune at the eastern end of the main slack
118 transect in October 2011. Core was delivered in 1 m lengths within a polythene sleeve;
119 recovery varied between 90 and 95%. The core was sub-sampled at 0.1 m intervals by slicing
120 through the sleeve with aliquots stored in airtight glass vials later being used to test an offline
121 preparation method for deuterium ($\delta^2\text{H}$) analysis (see 4.3 below). The hole remained open
122 during drilling with only the upper ~0.3 m being dry and friable. The remainder of the sand
123 was moist and comprised consistently fine-grained to silt-grade material. The hole did not
124 reach the water table but was lined with 36 mm diameter plastic pipe and capped top and
125 bottom to allow future access if required.

126

127 Four additional deep cored dipwells were hammer-drilled using a Cobra TT percussion drill
128 along the line of the main slack dipwell transect (Fig. 1) to depths up to 9m (Table 1) during
129 November 2011. Continuous sampling of the unsaturated zone was achieved in the first three
130 dipwells (D2, D3 and D4) with partial sampling in D5 nearest the shore. Small sub-samples

131 taken at 0.1 m intervals from the D2 and D4 cores were transferred into airtight glass vials for
132 $\delta^2\text{H}$ analysis of the sand moisture. All cored sections from D2, D3, and D4 were then sliced
133 into 0.2 m intervals from which about 40 mm was deposited into pre-weighed sealable
134 containers to measure gravimetric moisture content and the remainder transferred to sealed
135 plastic bags and refrigerated for subsequent centrifugation in the laboratory. Dipwells D3, D4
136 and D5 penetrated the water table, below which coring ceased to be effective. Piezometers
137 were completed and cased to below water level, where possible, with 1 m of permeable
138 casing at the bottom of the hole.

139

140 Owing to a problem of sand fall-in during drilling which affected the top sample of many of
141 the core runs, several samples from each piezometer had to be discarded, leaving a number of
142 small gaps in each of the resulting profiles (Section 4.3).

143

144 The sites were chosen to minimize the influence of disturbance by trees and their roots.
145 Details of vegetation at each site have been recorded (Table 1) from a vegetation survey that
146 took place in 2012.

147

148 Sand moisture contents were calculated from the weight loss observed after heating
149 subsamples to 75°C for 48 hours. The dried samples from D3 and D4 were subsequently used
150 for grain size analysis.

151

152 The bagged sands were refrigerated and centrifuged soon after returning from the field. Sub-
153 samples were transferred to centrifuge buckets made from inert material and centrifuged at
154 14,000 rpm for 25 minutes. The drained waters were passed through 0.45 μm filters and split
155 between two HDPE bottles per sample. One of each pair of bottles was acidified to 1% with
156 Aristar nitric acid for determination of cations. In addition, aliquots were taken for standard
157 $\delta^2\text{H}$ and $\delta^{18}\text{O}$ analysis from those samples which yielded sufficient volume. Specific
158 electrical conductivity (SEC) was determined on the unacidified sample splits.

159

160 Owing to ingress of fine silty sand during an initial attempt to sample groundwater standing
161 in D3, D4, and D5 the piezometers were re-drilled to a depth of 9.2 m (Table 1) and
162 completed with a 1 m, 36 mm diameter screen wrapped in a geotextile filter membrane
163 section at the bottom of the piezometer. This enabled low turbidity samples to be obtained
164 from $D_{\text{new}4}$ and $D_{\text{new}5}$, but the water column in $D_{\text{new}3}$ was too small to sample.

165 All piezometer groundwater samples, beneath both dune slack and high dune, were pumped
166 using a portable peristaltic pump and where feasible pH, Eh, and dissolved oxygen were
167 determined by electrodes in a flow-through cell. SEC and temperature (determined by
168 thermistor thermometer) were also measured. Sampling commenced when purging was
169 completed as indicated by stable field measurements, which sometimes involved emptying
170 the piezometer and allowing it to refill before sampling. Alkalinity as HCO_3 was measured on
171 site with a digital titrator. The bedrock borehole was artesian during sampling and was
172 sampled using the same methods as the piezometers.

173

174 The groundwaters from $D_{\text{new}4}$ and $D_{\text{new}5}$ along with shallow slack dipwells 1, 2 and 3, PR2
175 and the underlying Pilton Mudstone formation were sampled for major and minor ion
176 chemistry, stable isotopes and sulphur hexafluoride (SF_6).

177

178 Samples of groundwater were collected in pairs of HDPE bottles, one of which was acidified
179 to 1% with nitric acid, before refrigeration and transfer to the laboratory. Unfiltered
180 groundwater samples were collected for $\delta^{18}\text{O}$, $\delta^2\text{H}$ and $\delta^{13}\text{C}$ analysis. Samples for SF_6
181 (sulphur hexafluoride) measurement were collected by the displacement method into glass
182 bottles contained within metal cans to minimise atmospheric contamination (Oster 1994).

183

184 Grain size analysis was carried out on a Mastersizer 2000, which uses laser diffraction to
185 measure particle sizes. Selected grain samples were analysed by SEM. Determination of
186 major and minor ions was carried out using ICP-MS for cations and ion chromatography for
187 anions. Ionic balances were found to be within $\pm 10\%$, a relatively wide error band but most
188 likely due to the dilutions necessary for the analysis of these low-volume samples. Stable
189 isotopes were measured by isotope ratio mass spectrometry following offline preparation by
190 CO_2 equilibration ($\delta^{18}\text{O}$), zinc reduction ($\delta^2\text{H}$) and acidification with H_3PO_4 ($\delta^{13}\text{C}$ -TIC), with
191 precisions of $\pm 0.1\text{‰}$, $\pm 1\text{‰}$ and $\pm 0.2\text{‰}$ respectively. SF_6 analysis was performed by GC-ECD
192 following cryogenic pre-concentration, with a detection limit of 0.1 pmol/L.

193

194

195

196

197

198

199 **4. RESULTS**

200

201 **4.1 Grain size and mineralogy**

202

203 The grain size analysis profiles for D3 and D4 are consistent with a well-sorted average D_{10}
204 and D_{90} of 120 μm and 280 μm respectively, i.e. ‘very fine to medium sand’. No anomalous
205 silt or clay layers were penetrated. The full range of grain sizes within the profiles D_{10} and
206 D_{90} are from 97–320 μm (Fig. 3).

207

208 SEM analysis of selected grain samples (2.2 to 2.4 m in D2, 2.4 to 2.6 m in D3 and D4) are
209 consistently dominated by calcite derived from shell debris. The samples comprise Ca and
210 Mg-rich shell fragments and fossils, quartz grains coated with illite, smectite, chlorite and
211 thin iron coatings, with potassium and plagioclase feldspars and some faecal pellets.

212

213 **4.2 Unsaturated zone moisture content**

214

215 The gravimetric porewater profile in the unsaturated zones in the high dune (Fig. 4) shows
216 that dipwell D2 has a moisture content in the range 3–9% while D3 has 5–12%. The
217 unsaturated zone porewater profile for D4 is 5–11% to within ~ 0.5 m above the standing
218 water level, below which moisture content rises to between 21–24 % through the capillary
219 fringe.

220

221 **4.3 Unsaturated zone hydrochemistry and isotopes**

222

223 The major ion chemistry of the dune porewaters (Table 2) is variable, with total dissolved
224 solids (TDS) within the range 245–635 mg/l. The chemistry of the porewaters is dominated
225 by Ca and HCO_3 from the dissolution of shell debris, and is supplemented by variable
226 proportions of Na and Mg (cations) and Cl and SO_4 (anions) from marine aerosol sources.

227

228 Most stable isotope results for the unsaturated sands are restricted to $\delta^2\text{H}$ because the small
229 amount of sample usually available was only sufficient for the direct reduction technique
230 (based on that of Turner and Gailitis, 1988). These results are shown in Fig. 5. However, in
231 some cases both $\delta^2\text{H}$ and $\delta^{18}\text{O}$ could be measured on centrifuged water using standard

232 preparation methods. Values of $\delta^2\text{H}$ obtained in this way are included in Fig. 5, showing that
233 the results are generally comparable within measurement error to the direct reduction data.

234

235 **4.4 Saturated zone hydrochemistry, stable isotopes and sulphur hexafluoride**

236

237 The analytical results for the groundwater samples collected from below the dune slacks and
238 high dunes are supplemented by a sample from the bedrock (Pilton Mudstone Formation)
239 which is hydraulically isolated from the dune aquifer by estuarine clay. The major ion
240 chemistry for all groundwater samples shows anions are dominated by HCO_3 (Table 3). The
241 cations are dominated by Ca below the slacks 1, 2 and PR2, with increasing Na dominance
242 below high dune samples $D_{\text{new}4}$ and $D_{\text{new}5}$, dune slack 3 and the bedrock borehole.

243

244 O, H and C stable isotopes were measured on samples from the saturated zone in the high
245 dune $D_{\text{new}4}$ and $D_{\text{new}5}$ dipwells, dune slack PR2 and bedrock (Table 3).

246

247 SF_6 values (Table 4) are corrected for excess air (Darling et al. 2012) on the assumption that
248 this is present at 1.5 ccSTP/l, based on sand-column experiments of Holocher et al. (2002).
249 An excess air correction of 2.5 ccSTP/l is used for the sample from the Pilton Mudstone
250 Formation because of some uncertainty about the recharge mechanism. The SF_6 residence
251 times assume a mean annual air temperature of 10°C.

252

253

254 **5 DISCUSSION**

255

256 **5.1 The recharge process**

257

258 5.1.2 Unsaturated zone

259

260 Unsaturated zone Cl (Fig. 6) and $\delta^2\text{H}$ profiles (Fig. 5) appear to reflect the rate of infiltration
261 into the high dunes. A high Cl pulse normally occurs at the beginning of each autumn rainfall
262 period flushing dry deposition consisting mainly of Cl, Na and SO_4 from the summer period
263 into the newly infiltrating rain-fed recharge (Malcolm & Soulsby 2001). While Na and SO_4
264 are affected by sorption and other exchange processes Cl is more conservative and tends to
265 remain in the profile as a peak. However, the conventional pattern of dry summers and wet

266 winters is not consistent with recent notably wet summers in 2007 and 2008, and a
267 particularly wet July in 2009, all of which are likely to have perturbed the normal sequence to
268 some extent.

269

270 While there may be some ambiguity in the interpretation of the observed Cl peaks as
271 infiltration rate indicators, stable isotopes can also be used in this role. Colder winter rainfall
272 tends to have a more negative $\delta^2\text{H}$ composition than generally warmer summer rainfall. The
273 record from the nearest rainfall isotope monitoring station at Wallingford demonstrates this
274 (Fig. 5), with particularly negative compositions during the winters of 2008/09 and 2009/10.
275 Although Wallingford is approximately 150 km to the east (Fig. 1) and its rainfall has
276 undergone some relative depletion by the ‘continental effect’ (Darling and Talbot 2003), it is
277 likely to be broadly similar to the magnitude of the cyclicity at Braunton Burrows. Significant
278 variations in the $\delta^2\text{H}$ profiles due simply to near-surface evaporative fractionation appear to
279 be ruled out by the centrifuged porewater samples, whose $\delta^2\text{H}$ and $\delta^{18}\text{O}$ values plot on a slope
280 of ~ 6 (Fig. 7) rather than the 2–3 typical of soil moisture evaporation (Barnes and Allison,
281 1988).

282

283 Based on their apparent cyclicity, both the $\delta^2\text{H}$ and Cl profiles from D2 and D4 suggest a
284 moisture infiltration rate of 0.75 to 1 m/yr (Figs 5 and 6). Diffusion tends to blur the annual
285 cycles at greater depth. The cyclicity in the upper parts of the profiles clearly confirms that a
286 key transport mechanism in the unsaturated zone is piston flow (as new water arrives at the
287 top of the column, old water is displaced at the bottom and the whole column moves
288 uniformly downwards). The infiltration rate indicated by the Cl and $\delta^2\text{H}$ profiles in dipwells
289 D2 and D4 suggests that it would take 6–7.5 yr and 5–6 yr for infiltration to reach the water
290 table at D4 and D5 respectively.

291

292 However, the moisture infiltration rate of 0.75 to 1 m/yr suggested by the $\delta^2\text{H}$ and Cl profiles
293 from D2 and D4 should also be considered in the context of the moisture content data (Fig. 4)
294 and local meteorological data. The median moisture contents of D2 and D4 are $\sim 6\%$ and 8%
295 by weight respectively, implying volumetric water contents of $\sim 10\%$ and 13% based on a dry
296 bulk density for dune sand of $\sim 1600 \text{ kg/m}^3$ (Ritsema and Dekker, 1994). These volume
297 percentages translate to water contents of 100–130 mm for an infiltration rate of 1 m/yr.
298 Rainfall at Chivenor (5 km E of the dunes) over the five years preceding the month of
299 sampling averaged 925 mm/yr (based on data from

300 <http://www.metoffice.gov.uk/climate/uk/stationdata/chivenordata.txt>). Actual evapotranspiration
301 data from the local MORECS (Meteorological Office Rainfall and Evapotranspiration
302 Calculation System) Square 165 for the same period gives an average effective rainfall of
303 45%, implying an effective rainfall of ~400 mm/yr on the dunes, nearly all of which should
304 theoretically infiltrate owing to the very limited potential for runoff. The calculated profile
305 water contents would then amount to some 25–33% of the effective rainfall/recharge. While
306 there is some uncertainty over the true value of actual evapotranspiration for the dunes, it is
307 unlikely to be significantly different from the MORECS average. The disparity may be
308 explained by preferential flow, which can include macropore flow but also (and probably
309 more significant for sand) ‘unstable wetting’: for example a homogeneous dune sand
310 lysimeter experiment by Hendrickx and Dekker (1994) found that at a depth of ~0.5 m, the
311 sand volume was only patchily wetted after 4 months of rainfall totalling 400 mm. The
312 existence of such ‘fingering’ in natural dune sands seems likely but it would take many more
313 than the three profiles reported here to characterise satisfactorily.

314

315 The existence of preferential flow implied by the meteorological data would mean that much
316 of the infiltration to the water table was moving rather faster than the maximum rate of
317 1 m/yr implied by the profile fluctuations in Figs 5 and 6. This could still be occurring via
318 piston flow; the rather wetter profile D4 indicates a somewhat faster infiltration rate than the
319 drier D2 (Figure 5), so it may be that the rate rises proportionally with moisture content in
320 wetter fingers of sand.

321

322 5.1.3 Groundwater

323

324 Groundwater recharged during the past four decades can in principle be dated on the basis of
325 its SF₆ concentration given certain assumptions about likely recharge conditions, principally
326 mean annual air temperature but also the amount of excess air (EA) incorporated during
327 recharge (4.4 above). The residence times in Table 4 have been calculated on a ‘piston flow’
328 model of groundwater flow (Darling et al., 2012), though in reality most pumped
329 groundwater is a mixture of waters from all the flow lines reaching the discharge point, so the
330 ages given in Table 4 should be regarded as mean residence times (MRTs).

331

332 The results show that groundwater below the sampled high dunes had MRTs of ~13 and
333 ~16 yr, and below the dune slacks of ~6 yr. The greater thickness of the unsaturated zone

334 beneath the high dunes seems one obvious reason. There is, however, some uncertainty about
335 the lag on the SF₆ ‘clock’ during transit through the unsaturated zone (Darling et al. 2012),
336 therefore, some mixing with older stored waters could also be contributing. Simple binary
337 groundwater age mixing can often be detected by plotting SF₆ versus CFC
338 (chlorofluorocarbon) concentrations. However, owing to the reducing conditions in most of
339 the groundwaters, CFC analyses were not undertaken because of probable degradation effects
340 (Sebol et al. 2007).

341
342 The MRTs in the dune system can be compared to that of the Pilton Mudstone aquifer as
343 sampled at the Saunton Sands Golf Club (Bedrock BH, Fig. 1), which gives an MRT of
344 ~22 yr. As a locally confined aquifer this would be expected to contain older water than the
345 overlying dune system. While the calculated age is not much greater than those of the dunes
346 water, little is known of the turnover of the Pilton Mudstone aquifer or its excess air content
347 (see 4.4 above), which if higher than estimated would result in an older age.

348

349 **5.2 Evolution of water quality**

350

351 5.2.1 Unsaturated zone

352

353 The chemistry of the unsaturated zone porewaters (Table 2) derives from a variety of inputs.
354 Much of the Na, Cl and SO₄ must be derived from deposition of marine aerosols, but
355 superimposed on this are contributions from the mineralogy of the sand including calcareous
356 shell debris and fossiliferous calcite, quartz coated with illite, smectite, chlorite and Fe
357 compounds as well as potassic and plagioclase feldspars. Variable dissolution of these
358 minerals accounts for most of the fluctuations in the minor element hydrochemistry of the
359 dune porewaters. The lack of any rise in SO₄ with depth confirms the rather limited
360 mineralogical evidence (see 4.1 above) for the absence of pyrite in the dune sands, which
361 would tend to oxidise to sulphate.

362

363 The carbonate system is more consistent. The Mg/Ca molar ratios found in the porewaters of
364 piezometers D2, D3 and D4 increase with depth (Fig. 8) reflecting increasing Mg dissolution.
365 The near-constant Sr/Ca ratios (Fig. 9) suggest that incongruent dissolution of calcite is not
366 the cause and that the increased Mg is coming from another source, probably the Mg-rich
367 shell debris.

368 5.2.2 Groundwater

369

370 The groundwaters in the shallow sand aquifer continue to show the influence of mineralogy
371 and marine aerosols. The carbonate system again dominates the chemistry seen in the
372 groundwaters, most markedly at the slacks BB1, BB2 and PR2. These groundwaters are more
373 carbonate-dominated than the porewaters. Increasing influence of marine aerosols as Na and
374 Cl is seen below the high dunes and slack BB3 putting them closer within the main group of
375 porewaters (table 2). Dune slack BB3 is seen to behave slightly differently to the others
376 slacks; its higher marine aerosol signal may be due to its proximity to the sea.

377

378 The Mg/Ca molar ratios for the D4 and D5 groundwaters (Fig. 8) highlight their consistency
379 with the porewaters as they plot as a continuation of the porewater series. Mg is seen to
380 increase with depth as with the porewaters. The Sr/Ca ratios of the groundwaters (Fig. 9) are,
381 however, lower than those of the porewaters with an increase in Sr possibly consistent with
382 the occurrence of incongruent dissolution of calcite.

383

384 The high Fe and Mn present in the groundwaters beneath the slacks (PR2, BB1 and BB2) and
385 high dunes are a consequence of the reducing conditions illustrated by the dissolved oxygen
386 and Eh values. Both Fe and Mn are found as dissolved ions due to the reduction of iron oxide
387 and manganese oxide mineral coatings and minerals found within the sand grains. This is in
388 contrast to the low Fe and Mn concentrations found in the porewaters. The exception to this
389 is the dune slack groundwater BB3 with Fe and Mn concentrations comparable to the dune
390 porewaters. Although the dissolved oxygen is again low in this sample, the redox is elevated,
391 this together with the low Fe and Mn points to a more oxygenated sample as with the
392 porewaters. It is likely that a greater amount of recharge occurs through the flooded slacks
393 than beneath the dunes (D Clarke, personal communication), and this may be a more recent
394 recharge signal (BB3 gives the youngest MRT). The proximity of BB3 to the sea may
395 account for the raised SEC and increased marine aerosol signal.

396

397 Groundwater samples from the dipwells D4 and D5 and dune slack piezometer PR2 gave
398 $\delta^{13}\text{C}_{\text{TIC}}$ values of -9.5 , -9.3 and -8.9 ‰ respectively. The similarity of the values suggests
399 rather consistent carbonate system conditions in the dune groundwaters. The total inorganic
400 carbon (TIC) in the groundwaters beneath the dunes is likely to arise from reaction between
401 shelly fragments in the sand and the CO_2 generated by soil bacterial respiration. Reaction

402 between soil CO₂ (~-26‰) and marine-derived calcite (~0‰) initially results in a δ¹³C_{TIC}
403 value of ~-13‰. Subsequent dissolution-reprecipitation processes will tend to drive the
404 value towards the calcite composition, making it less negative as observed in the dune sand
405 groundwaters. However, this can only occur under closed-system conditions, i.e. no further
406 supply of soil CO₂. This is consistent with the commencement of the SF₆ “clock” well above
407 the water table lying at the base of the unsaturated zone (5.1.2 above). The evolution of the
408 δ¹³C_{TIC} from initial equilibrium of ~-13‰ requires a certain amount of time, so the MRTs
409 indicated by SF₆ (13 and 16 yr respectively) are consistent with this interpretation.
410 Methanogenesis, an alternative explanation for the shift in δ¹³C_{TIC} via co-produced
411 isotopically heavy CO₂ (Stuyfzand 1993) can be ruled out on the basis of detectable NO₃ and
412 absence of evidence for SO₄ reduction (Table 3), backed up by measurements of dissolved
413 CH₄ in two slack groundwaters (PR2 and Orchid) which were both extremely low at <1 µg/L.

414

415 By comparison, the Pilton Mudstone formation gave δ¹³C_{TIC} values of -13.6 ‰ which would
416 be consistent with relatively young groundwaters in a locally confined aquifer.

417

418 Nitrate concentrations in the unsaturated zone and the groundwaters are generally low, the
419 only exception to this being the top (0–200 mm) section of D2 and D3 which have 33 and
420 120 mg l⁻¹ NO₃ respectively. (The top 50 mm of D4 was unavailable for sampling which may
421 explain the lack of a high NO₃ concentration being found in this profile.) The elevated NO₃ at
422 the top of the soil zone may be a consequence of atmospheric deposition along with plant and
423 animal inputs as all material was used to provide porewater. Nitrate concentrations within the
424 underlying bedrock aquifer (Pilton Mudstone Formation) are also low.

425

426

427 **6 CONCLUSIONS**

428

429 This study of a coastal dune system in SW England has used a range of environmental tracers
430 to address the four key questions posed in the Introduction.

431

432 First, while this study has found evidence for the existence of piston flow through the
433 unsaturated zone, the imbalance between indicated and likely recharge rates points to the
434 existence of some preferential flow, probably mainly due to unstable wetting rather than
435 macropore flow, which would seem less likely to be significant in a dunes context. It may be

436 the case that even in locally wetter zones, piston flow still predominates, but at a faster rate.
437 To get a better indication of this, a higher density of unsaturated zone profiling would be
438 required.

439

440 Second, water quality in the unsaturated zone of the dunes aquifer is predominantly the result
441 of the deposition of marine aerosols and the dissolution of shell fragments. There appears to
442 be relatively little reaction with the sand matrix. Saturated zone water quality largely matches
443 porewater compositions at the base of the unsaturated zone, implying that if faster infiltration
444 routes exist, the chemistry of these waters has already evolved a similar chemistry.

445

446 Third, it appears that the main hydrochemical evolution of unsaturated zone porewater occurs
447 very rapidly, in months rather than years. This is because comparatively rapid processes like
448 the mobilization of surface salt crusts and the dissolution of shell calcite tend to dominate the
449 water quality. However, minor changes like the slow build-up of Mg take longer because of
450 the reaction kinetics. The main change in the underlying groundwater is that the low-O₂
451 conditions appear to be slowly reducing the concentrations of ions like SO₄ and NO₃ and
452 increasing the concentrations of Fe and Mn, while also favouring the mineralisation of
453 carbon. Incongruent mobilisation of Mg continues. Measured mean residence times of up to
454 16 yr indicate that dissolved O₂ is relatively persistent with time, suggesting that the bacterial
455 mediation of reducing reactions is not highly developed.

456

457 Fourth, while this study did not include a water quality monitoring element, certain
458 conclusions can be drawn about the effects of secular changes in conditions, whether climatic
459 or morphological. Gradual changes in mean rainfall and temperature are unlikely to affect
460 water quality significantly, but changes in the supply of marine salts (e.g. via much stormier
461 conditions) or the supply of shell fragments (e.g. because of dune migration) could have a
462 rather greater impact on water quality.

463

464 The results of this study are applicable to other unmodified dune spit systems and hence their
465 future environmental management.

466

467

468

469

470 **Acknowledgments**

471 The authors acknowledge the assistance of Ned Hewitt (CEH), Ian Woods (BGS) and
472 Martin Hollingham (independent) for help in installing piezometers. Derek Clarke
473 (Southampton University) is thanked for sharing his knowledge of dune systems as is Antoni
474 Milodowski (BGS) for SEM of the sand grains. BGS and CEH labs at both Wallingford and
475 Keyworth are thanked for the analytical results. Sam Amy (CEH) is thanked for vegetation
476 classification data. MORECS data is licensed under Crown Copyright from the UK Met
477 Office (010045532). The reviewers are thanked for their constructive comments and ideas.
478 DA, WGD, NSR, and PJW publish with the permission of the Executive Director, British
479 Geological Survey (NERC).

480

481 **REFERENCES**

- 482 Barnes, C.J., Allison, G.B. 1988. Tracing of water movement in the unsaturated zone using
483 stable isotopes of hydrogen and oxygen. *J. Hydrol.* 100, 143–76. doi: 10.1016/0022-
484 1694(88)90184-9
- 485 Burden, R.J. 1988. A hydrological investigation of three Devon sand dune systems: Braunton
486 Burrows, Northam Burrows and Dawlish Warren. PhD Thesis, University of Plymouth.
- 487 Clarke, D., Sanitwong Na Ayutthaya, S. 2010. Predicted effects of climate change, vegetation
488 and tree cover on dune slack habitats at Ainsdale on the Sefton Coast, UK. *J Coast Conservat*
489 14, 115–25. doi: 10.1007/s11852-009-0066-7
- 490 Curreli, A., Wallace, H., Freeman, C., Hollingham, M., Stratford, C., Johnson, H., Jones, L.
491 2013. Eco-hydrological requirements of dune slack vegetation and the implications of climate
492 change. *Science of the Total Environment* 443, 910–919. doi:
493 10.1016/j.scitotenv.2012.11.035
- 494 Darling, W.G., Talbot, J.C. 2003. The O & H stable isotopic composition of fresh waters in
495 the British Isles. 1. Rainfall. *Hydrology & Earth System Sciences* 7, 163–181.
- 496 Darling, W.G., Bath, A.H., Talbot, J.C. 2003. The O & H stable isotopic composition of fresh
497 waters in the British Isles. 2. Surface waters and groundwater. *Hydrology & Earth System*
498 *Sciences* 7, 183–195.
- 499 Darling, G. Goody, D.C. MacDonald, A.M., Morris, B.L. 2012. The practicalities of using
500 CFCs and SF₆ for groundwater dating and tracing. *Applied Geochemistry* 27. 1688–1697.
501 doi: 10.1016/j.apgeochem.2012.02.005
- 502 Davy, A.J., Grootjans, A.P., Hiscock, K., Petersen, J. 2006. Development of eco-hydrological
503 guidelines for dune habitats - Phase 1. English Nature Reports, Number 696.
- 504 Davy, A.J., Hiscock, K.M., Jones, M.L.M., Low, R., Robins, N.S., Stratford, C.J. 2010.
505 Ecohydrological guidelines for wet dune habitats – Phase 2. Environment Agency Report.
- 506 Doody, J.P. 2008. Sand dune inventory of Europe, 2nd edn. National Coastal Consultants and
507 EUCC - The Coastal union, in association with the IGU Coastal Commission, Peterborough.
- 508 Grootjans, A.P., Sival, F.P., Stuyfzand, P.J. 1996. Hydro-geochemical analysis of a degraded
509 dune slack. *Vegetatio* 126, 27–38.
- 510 Grootjans, A.P., Ernst, W.H.O., Stuyfzand, P.J. 1998. European dune slacks: strong
511 interactions of biology, pedogenesis and hydrology. *Tree* 3, 96–100.
- 512 Hendrickx, J.M.H., Dekker, L.W. 1991. Experimental evidence of unstable wetting fronts in
513 non-layered soils. In: *Proc. Natl. Symp. on Preferential Flow*. Chicago, Ill. 16–17, Dec. 1991,
514 St. Joseph, Mich.: Am. Soc. Agric. Eng., 22–31.

515 Holocher, H., Peeters, F., Aeschbach-Hertig, W., Hofer, M., Brennwald, M., Kinzelbach, W.,
516 Kipfer, R. 2002. Experimental investigations on the formation of excess air in quasi-saturated
517 porous media. *Geochimica et Cosmochimica Acta* 66, 4102–4117. doi: 10.1016/S0016-
518 7037(02)00992-4

519 Malcolm, R., Soulsby, C. 2001. Hydrogeochemistry of groundwater in coastal wetlands:
520 implications for coastal conservation. *Science of the Total Environment* 265, 269–280. doi:
521 10.1016/S0048-9697(00)00663-X

522 Oster, H. 1994. Datierung von Grundwasser mittels FCKW: Voraussetzungen, Möglichkeiten
523 und Grenzen, Dissertation, Inst. für Umweltphys., Universität Heidelberg.

524 Ritsema, C.J., Dekker, L.W. 1994. Soil moisture and dry bulk density patterns in bare dune
525 sands. *Journal of Hydrology* 154, 107–131.

526 Robins, N.S., Jones, M.L.M. 2013. Ecohydrological ‘Indicators of alteration’ - a robust
527 measure of change in dune slacks. *Ecohydrology* 6, 256–263. doi: 10.1002/eco.1264

528 Robins, N.S., Pye, K., Wallace, H. 2013. Dynamic coastal dune spit: the impact of
529 morphological change on dune slacks at Whiteford Burrows, South Wales, UK. *Journal of*
530 *Coastal Conservation* 17, 473–482. doi: 10.1007/s11852-013-0245-4

531 Saye, S.E., Pye, K. 2007. Implications of sea level rise for coastal dune habitat conservation
532 in Wales, UK. *Journal of Coastal Conservation* 11, 31–52. doi: 10.1007/s11852-007-004-5

533 Sebol, L.A., Robertson, W.D., Busenberg, E., Plummer, L.N., Ryan, M.C., Schiff, S.L. 2007.
534 Evidence of CFC degradation in groundwater under pyrite-oxidizing conditions. *J. Hydrol.*
535 347, 1–12. doi: 10.1016/j.jhydrol.2007.08.009

536 Sival, F.P., Strijkstra-Kalk, M. 1999. Atmospheric deposition of acidifying and
537 eutrophating substances in dune slacks. *Water Air Soil Pollut.* 116, 461–77.

538 Stratford, C., Robins, N.S., Clarke, D., Jones, M.L.M. Weaver, G. 2013. An ecohydrological
539 review of dune slacks on the west coast of England and Wales. *Ecohydrology* 6, 162–171.
540 doi: 10.1002/eco.1355.

541 Stuyfzand, P. J. 1989. A new hydrochemical classification of watertypes. *IAHS Publ* 182,
542 89–98.

543 Stuyfzand, P.J. 1993. Hydrochemistry and hydrology of the coastal dune area of the western
544 Netherlands. PhD thesis, Vrije Universiteit Amsterdam.

545 Turner, J.V., Gailitis, V. 1988. Single-step method for hydrogen isotope ratio measurement of
546 water in porous media. *Analytical Chemistry* 60, 1244–1246. doi: 10.1021/ac00162a030

- 547 Vandenbohede, A. Luyten, K. Lebbe, L. 2008. Effects of Global Change on Heterogeneous
548 Coastal Aquifers: A Case Study in Belgium. *Journal of Coastal Research* 24, 160 – 170.
549 doi:10.2012/05-0447.1
- 550 Van der Hagen, H.G.J.M., Geelen, L.H.W.T., de Vries, C.N. 2008. Dune slack restoration in
551 Dutch mainland coastal dunes. *Journal for Nature Conservation* 16, 1–11.
552 doi:10.1016/j.jnc.2007.03.004
- 553 Willis, A.J., Folkes, B.F., Hope-Simpson, J.F., Yemen, E.W. 1959. Braunton Burrows: the
554 dune system and its vegetation. Parts 1 and 2. *Journal of Ecology* 47, 1–24 and 249–288.

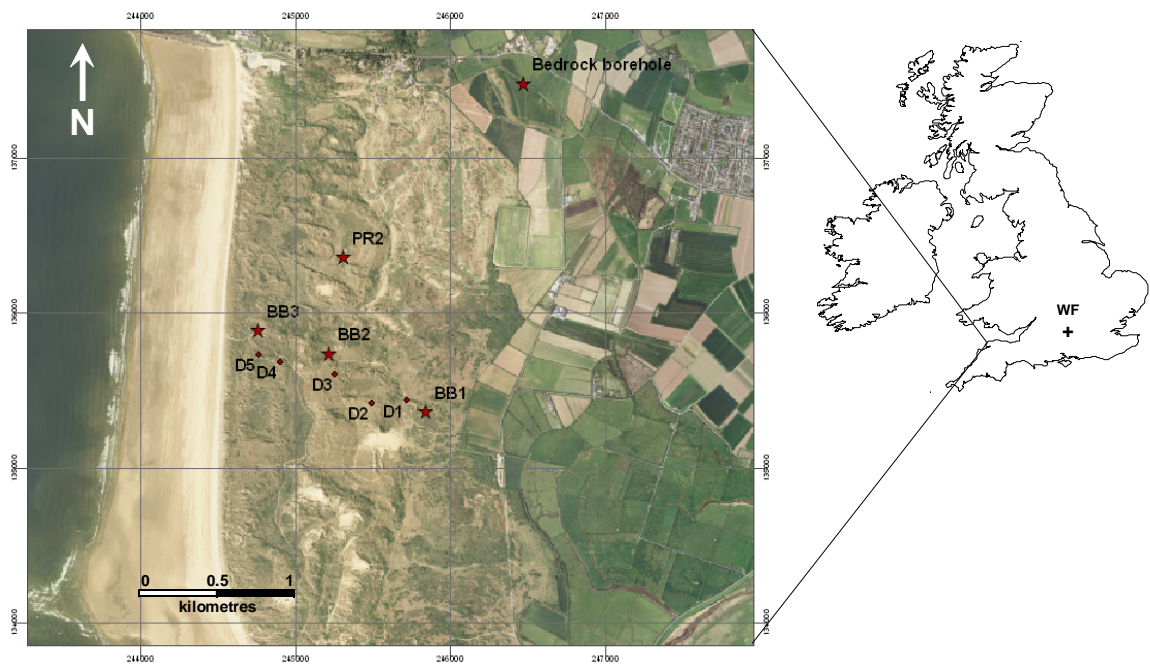


Figure 1. Map of Branton Burrows, SW England, with key sites marked. Location of Wallingford (WF) shown on inset map. Based upon aerial photography from © NextPerspectives.

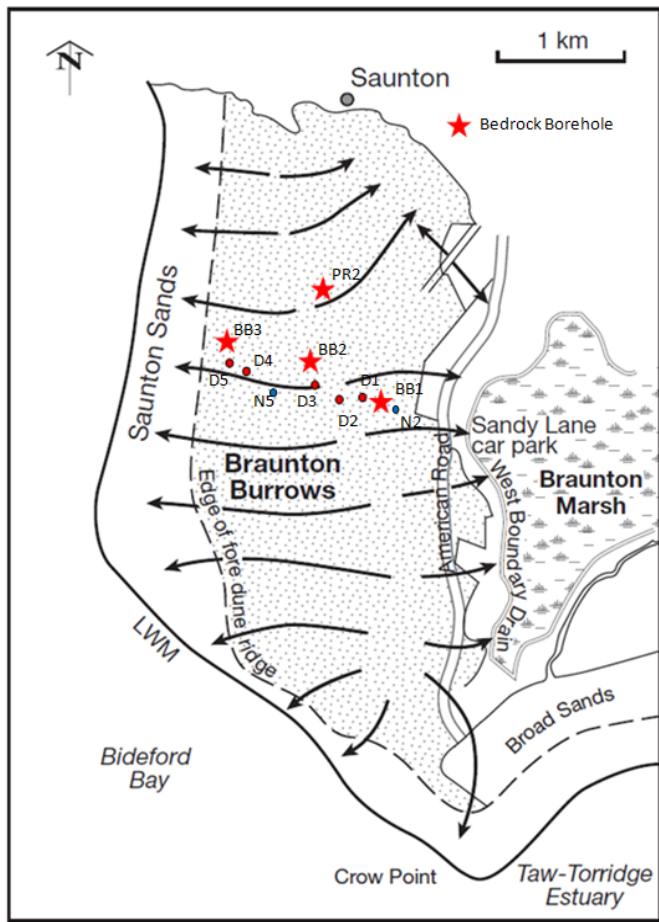


Figure 2. Conceptual groundwater flow at Braunton Burrows from Stratford et al (2013).

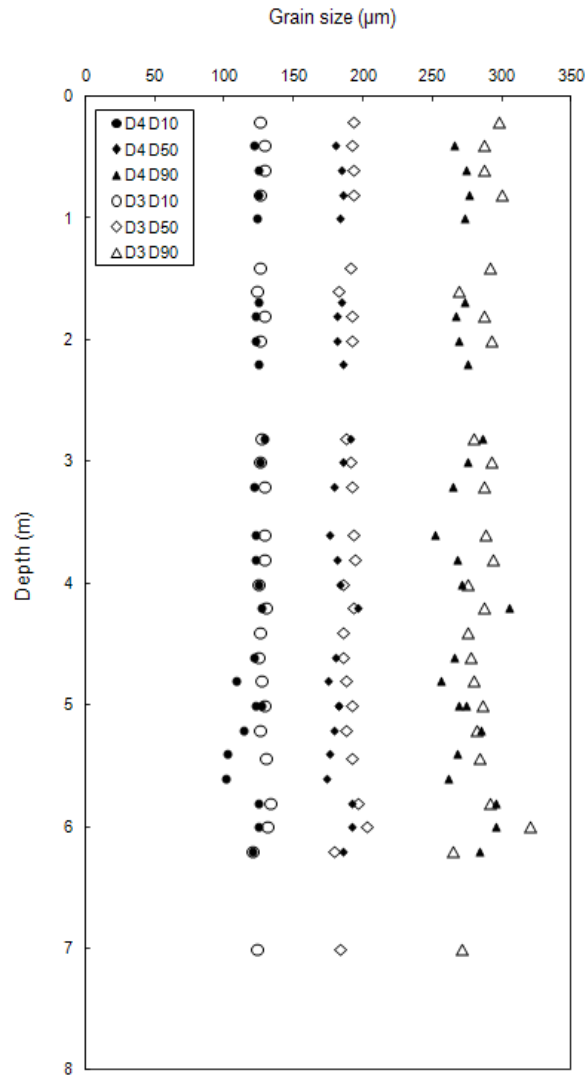


Figure 3. Results of grain size analysis for D4 showing D_{10} , D_{50} , and D_{90} .

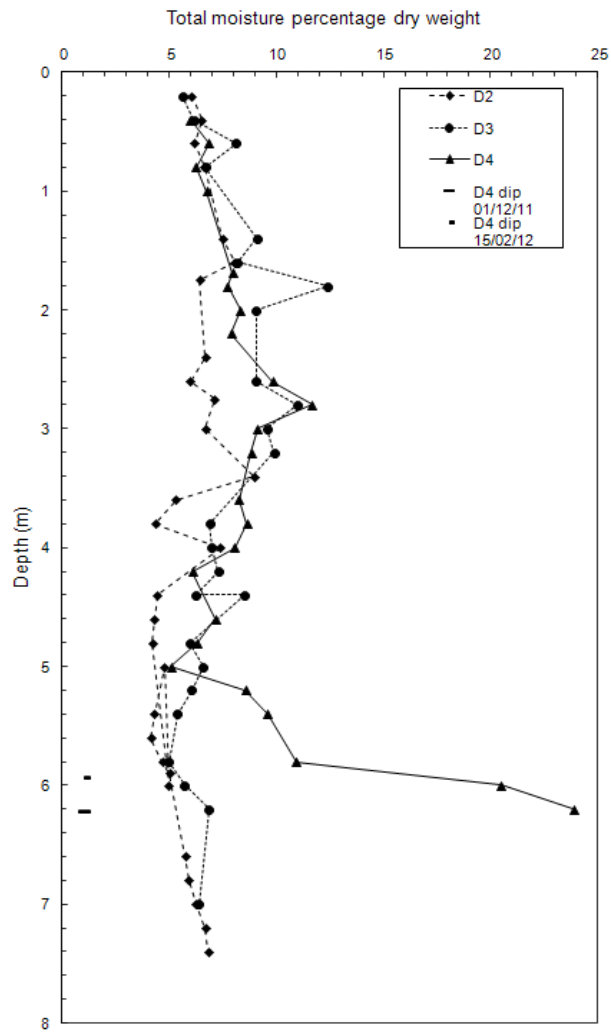


Figure 4. Moisture content depth profiles for piezometers D2, D3 and D4 showing water table in D4 in December 2011 and February 2012.

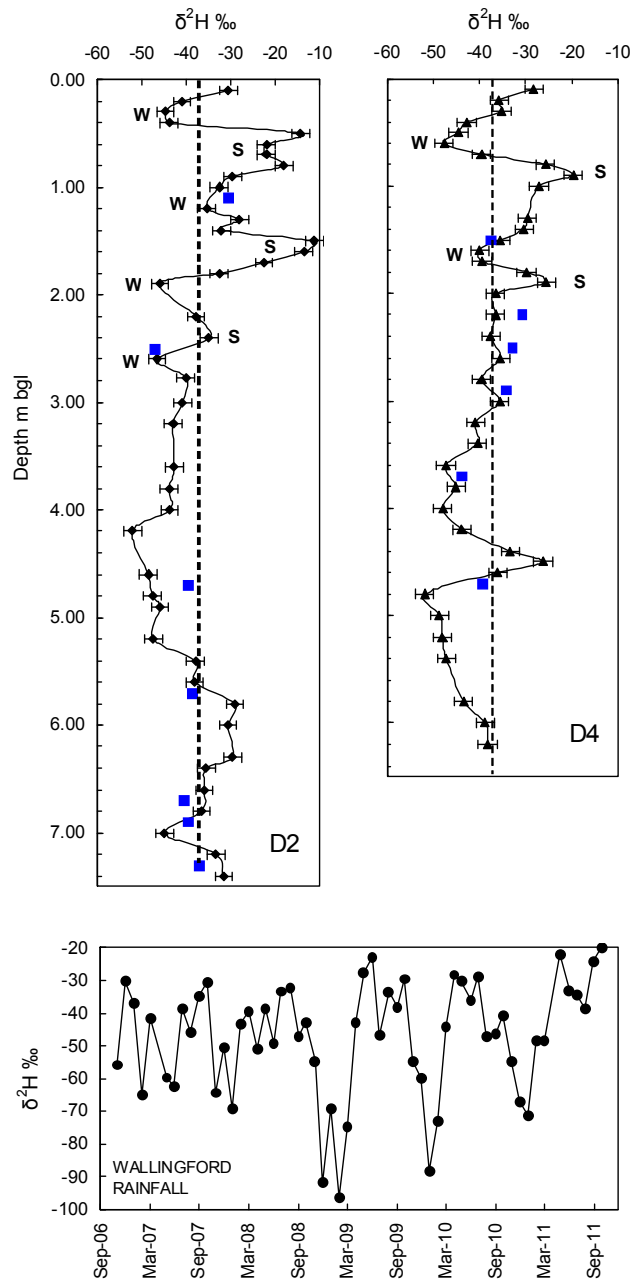


Figure 5. Profiles of $\delta^2\text{H}$ in sand moisture from piezometers D2 and D4, autumn 2011. Square datapoints represent analyses of water extracted by centrifuge, showing generally good agreement with the directly reduced sand moisture. Also shown is the rainfall isotope record from Wallingford (nearest rainfall isotope collection station) for the previous five years. The dashed vertical line shows the approximate $\delta^2\text{H}$ composition of the underlying groundwater. Probable summer (S) and winter (W) peaks and troughs are identified on the profiles.

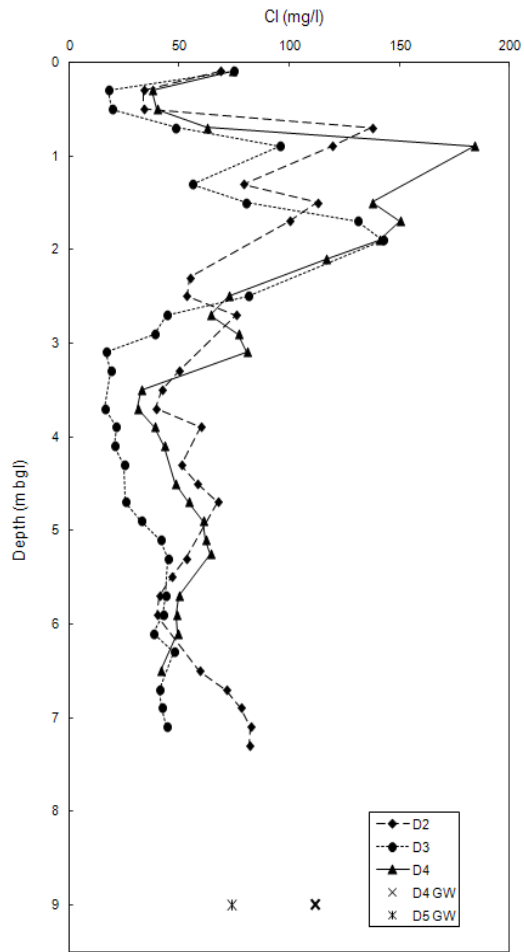


Figure 6. Concentration of chloride (mg/l) in the unsaturated zone below the high dunes. Data from centrifuged porewaters.

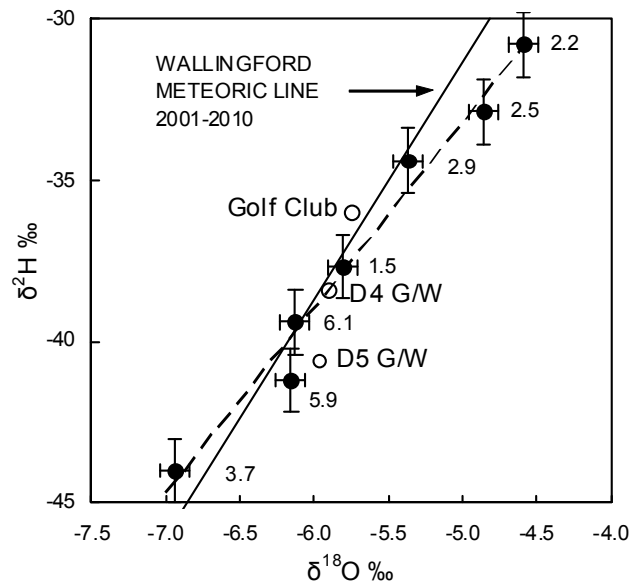


Figure 7. Isotopic co-plot showing the composition of centrifuged waters from the D4 profile compared to the meteoric line at Wallingford (WML), the nearest available GNIP network station (data from <http://www.univie.ac.at/cartography/project/wiser/index.php>). Sample depths are given in m bgl. Pumped groundwaters from piezometers D4 and D5 and the Golf Club (bedrock aquifer borehole) are also included. The lack of significant deviation from the WML suggests that evaporation has little effect on the infiltrating water.

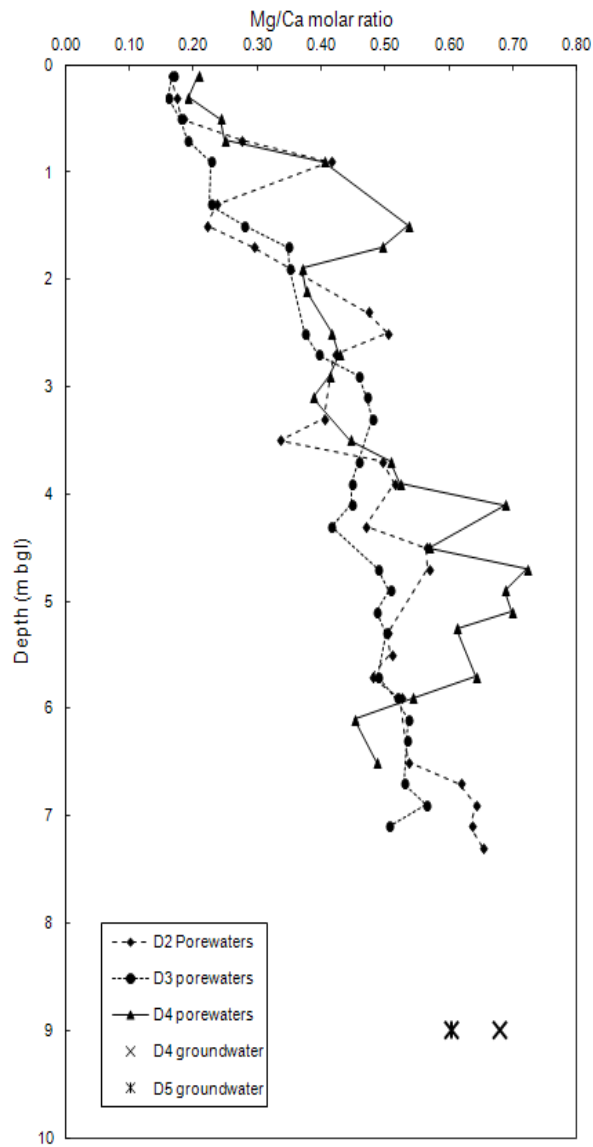


Figure 8. Mg/Ca molar ratios for the porewaters and groundwaters of the high dunes. Groundwaters were sampled from approximately 9 m bgl.

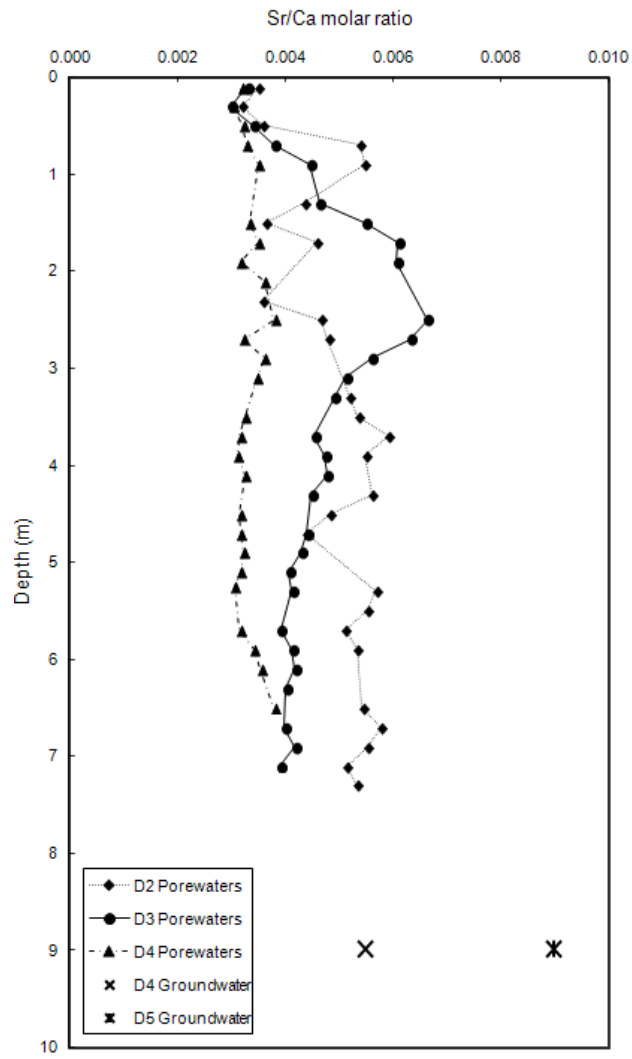


Figure 9. Porewater Sr/Ca molar ratio with depth.

Table 1. Construction details of sampled dune slack and high dune piezometers at Braunton Burrows, with water levels in mbgl (below ground level) at the time of sampling.

Dipwell	Surface elev. (m)	Drilled Depth (m)	Water level (mbgl)	Vegetation	Notes
BB1	9.75	1.97	top of casing	SD14 wet calcareous slack type	Dune slack
BB2	9.76	1.97	0.51	SD16 dry calcareous type	Dune slack
BB3	6.93	1.97	0.35	SD16 + SD14 slack-dry transitional	Dune slack
PR2	9.42	2.52	0.79	SD16 dry calcareous type	Dune slack
D1	16.14	6.00	Dry	Fixed dune vegetation	
D2	25.20	8.62	Dry	Fixed dune vegetation	
D3	17.03	8.62		Fixed dune vegetation	
Dnew3	17.03	9.20	8.38	Fixed dune vegetation	
D4	13.09	8.62		Fixed dune vegetation	Casing removed
Dnew4	13.09	9.20	5.93	Fixed dune vegetation	
D5	11.30	8.80		Fixed dune vegetation	Sediments risen to 5.93 mbgl by 17-Oct-12
Dnew5	11.30	9.20	5.1	Fixed dune vegetation	

Table 2. Major, selected minor and trace element analyses of dune porewaters from dipwells D2, D3 and D4.

Depth	SEC	Ca	Mg	Na	K	HCO ₃	Cl	SO ₄	NO ₃ -N	NO ₂ -N	Si	Fe _{tot}	Mn	Sr	PO ₄ -P
mbgl	μS cm ⁻¹	mg l ⁻¹	mg l ⁻¹	mg l ⁻¹	mg l ⁻¹	mg l ⁻¹	mg l ⁻¹	mg l ⁻¹	mg l ⁻¹	mg l ⁻¹	mg l ⁻¹	μg l ⁻¹	μg l ⁻¹	μg l ⁻¹	μg l ⁻¹
<i>Dipwell D2</i>															
0.1	605	79.8	7.99	33.9	11.8	171	68.4	74.7	8.90	0.088	1.93	33	13.7	612	180
0.3	478	45.5	4.78	52.0	3.09	182	33.9	19.7	4.46	0.045	2.07	9	2.7	318	<30
0.5	432	46.2	5.11	36.6	2.65	178	33.5	18.0	1.33	0.033	2.00	13	0.6	363	34
0.7	648	70.7	11.8	37.3	1.58	122	138	18.9	1.38	<0.006	3.00	4	3.8	834	<50
0.9	635	61.5	15.5	41.7	1.70	153	119	24.1	0.964	<0.006	3.15	<2	22	736	<50
1.3	522	56.6	8.11	29.9	1.31	133	78.9	13.4	0.773	<0.003	2.31	<2	4.8	539	<30
1.5	570	68.6	9.17	25.2	1.47	101	113	13.6	0.900	<0.006	2.32	3	3.1	545	<50
1.7	562	57.6	10.3	36.1	1.33	124	99.7	12.5	0.756	<0.003	2.00	<6	1.50	578	42
2.3	529	52.7	15.1	58.8	2.90	166	54.5	29.2	2.12	0.035	2.12	<2	4.2	414	45
2.5	491	37.7	11.5	49.0	1.69	155	53.4	21.4	0.959	0.029	3.24	<2	6.0	385	47
2.7	548	49.1	12.5	48.5	1.60	165	75.5	18.7	0.694	0.031	3.20	<2	14.9	514	<30
3.3	489	44.7	11.0	47.7	1.83	168	50.0	22.7	1.20	0.022	3.11	7	3.7	508	42
3.5	423	43.4	8.81	34.8	1.38	150	42.0	18.3	1.31	0.026	2.92	<2	6.6	507	42
3.7	463	37.4	11.2	44.5	1.73	158	39.4	26.9	2.07	0.029	3.12	2	5.6	483	46
3.9	505	38.8	12.1	48.9	2.20	161	59.5	27.6	1.19	0.033	3.00	<4	5.6	465	<30
4.3	512	40.9	11.6	51.7	2.14	174	50.7	27.0	1.69	0.037	4.00	<4	1.50	501	77
4.5	535	39.9	13.7	56.4	2.31	164	58.3	28.8	1.72	<0.003	4.00	<4	0.9	422	47
4.7	559	47.7	16.4	68.5	2.86	162	67.3	32.9	1.94	0.027	2.00	<4	1.6	459	55
5.3	497	43.3	13.2	44.8	2.17	162	53.0	23.3	1.64	0.031	3.46	<2	1.4	537	81
5.5	475	38.6	11.9	44.0	2.13	151	46.4	25.7	1.77	0.025	3.00	<4	2.4	467	58
5.7	470	53.1	15.4	51.3	2.51	182	40.8	23.2	1.59	0.025	4.00	<4	2.0	594	<30
5.9	428	36.8	11.7	37.4	1.86	147	40.0	23.7	1.21	0.029	3.26	<2	1.2	430	77
6.5	574	46.4	15.1	52.1	3.11	188	59.2	32.8	1.94	0.039	3.93	<2	1.2	551	65
6.7	538	38.7	14.5	51.4	2.68	150	71.5	27.8	1.52	<0.003	3.50	9	0.9	489	55
6.9	578	42.9	16.7	52.2	2.77	166	77.9	29.6	1.60	0.028	3.50	<2	0.9	519	49
7.1	598	44.1	17.0	53.2	2.42	156	82.5	32.1	2.11	0.027	3.21	4	1.3	495	68
7.3	600	45.2	17.9	53.9	3.01	167	81.8	32.1	1.47	0.024	3.62	<2	1.0	527	63
Mean	550	50.5	12.4	47.6	2.86	162	68.8	28.7	2.12	0.037	3.02	5	4.1	526	61
Min	423	36.8	4.78	25.2	11.8	101	33.53	12.5	0.69	<0.003	1.09	<2	0.6	309	<30
Max	873	90.1	17.88	68.5	9.60	238	137.6	74.7	8.90	0.153	4.00	33	22	966	81

Table 2 (contd). Major, selected minor and trace element analyses of dune porewaters from dipwells D2, D3 and D4.

Depth mbgl	SEC $\mu\text{S cm}^{-1}$	Ca mg l^{-1}	Mg mg l^{-1}	Na mg l^{-1}	K mg l^{-1}	HCO ₃ mg l^{-1}	Cl mg l^{-1}	SO ₄ mg l^{-1}	NO ₃ -N mg l^{-1}	NO ₂ -N mg l^{-1}	Si mg l^{-1}	Fe _{tot} $\mu\text{g l}^{-1}$	Mn $\mu\text{g l}^{-1}$	Sr $\mu\text{g l}^{-1}$	PO ₄ -P $\mu\text{g l}^{-1}$
<i>Dipwell D3</i>															
0.1	820	109	11.1	48.1	11.0	204	74.4	30.4	32.7	0.078	4.80	34	14.3	780	<30
0.3	427	45.4	4.94	27.8	4.2	188	17.8	14.8	6.00	0.027	2.21	4	1.0	381	61
0.5	362	49.9	5.77	39.3	2.6	169	19.3	11.6	1.53	0.025	2.42	2	0.6	337	67
0.7	466	57.4	7.94	42.4	2.0	168	48.4	14.7	0.724	0.024	2.37	<2	0.6	413	59
0.9	571	84.8	10.2	51.7	16.1	149	95.4	14.0	0.370	0.105	4.25	3	1.6	560	44
1.3	469	50.4	6.92	40.6	1.6	166	56.0	10.2	0.509	0.023	2.14	22	1.0	511	50
1.5	539	57.2	9.72	34.1	1.3	165	80.3	12.0	0.503	0.023	2.84	<2	0.9	684	47
1.7	585	60.8	12.9	28.0	1.4	135	130.7	16.5	0.616	<0.006	2.57	<2	0.6	809	88
1.9	646	68.1	14.4	32.2	1.8	145	142.3	15.6	0.615	<0.006	2.97	3	1.1	903	94
2.5	550	60.3	13.7	29.7	1.5	169	81.0	13.4	0.519	0.023	2.89	<2	0.4	874	42
2.7	491	55.1	13.2	26.7	1.4	173	44.3	10.5	0.362	<0.003	2.88	<2	0.3	761	62
2.9	439	44.0	12.2	24.9	1.3	192	39.0	12.1	0.445	0.023	2.72	<2	0.2	539	56
3.1	341	33.2	9.51	22.2	1.1	167	16.7	12.0	0.816	0.023	2.40	<2	0.7	372	48
3.3	372	39.1	11.4	24.2	1.4	183	19.0	11.6	0.375	<0.003	2.80	<2	0.7	420	49
3.7	370	35.9	9.97	25.5	1.5	183	16.1	14.1	0.940	0.024	3.07	<2	0.7	357	67
3.9	381	37.7	10.2	29.2	1.5	174	21.4	14.4	1.10	0.030	2.87	2	1.1	390	53
4.1	386	37.5	10.2	29.9	1.7	182	20.6	14.2	1.10	0.032	3.15	4	0.9	392	51
4.3	392	37.5	9.46	32.5	1.4	164	25.1	17.3	1.39	0.029	2.91	3	0.9	368	75
4.7	407	38.6	11.5	29.0	1.7	190	25.3	14.8	1.11	0.026	2.85	<2	1.4	371	51
4.9	451	43.1	13.3	33.0	2.0	201	32.6	15.7	1.04	0.026	3.05	<2	1.2	405	52
5.1	452	40.6	12.0	38.2	2.1	172	41.7	19.6	1.36	0.035	2.94	<2	1.5	362	55
5.3	460	40.0	12.2	33.3	2.1	170	44.6	19.2	1.07	0.040	2.75	9	1.2	360	49
5.7	492	42.7	12.7	42.6	2.4	194	43.7	21.1	1.26	0.040	3.23	3	0.9	366	69
5.9	456	40.1	12.6	44.1	2.4	166	42.6	21.9	1.40	0.034	2.97	7	1.3	361	59
6.1	463	38.3	12.5	39.0	2.5	184	38.3	19.0	1.14	0.031	3.10	<2	0.7	351	61
6.3	477	39.4	12.8	40.4	2.3	173	47.8	21.1	0.851	0.030	2.84	<2	0.7	346	64
6.9	467	38.9	13.3	41.3	2.6	176	41.9	21.6	2.03	0.029	2.95	3	1.1	355	64
7.1	487	39.6	12.2	42.6	2.8	180	44.0	23.6	1.57	0.031	3.30	<2	0.6	338	58
Mean	496	49.5	11.19	35.9	2.86	179	50.9	19.5	2.61	0.032	2.94	4.38	1.44	497.1	57
Min	341.1	33.2	4.9	22.2	1.1	135	16.1	10.2	0.36	<0.003	1.2	<2	0.2	337	<30
Max	820	108.5	14.78	54.5	16.1	261	142	70.4	32.65	0.105	4.80	34	14.3	902.5	94

Table 2 (contd). Major, selected minor and trace element analyses of dune porewaters from dipwells D2, D3 and D4.

Depth mbgl	SEC $\mu\text{S cm}^{-1}$	Ca mg l^{-1}	Mg mg l^{-1}	Na mg l^{-1}	K mg l^{-1}	HCO ₃ mg l^{-1}	Cl mg l^{-1}	SO ₄ mg l^{-1}	NO ₃ -N mg l^{-1}	NO ₂ -N mg l^{-1}	Si mg l^{-1}	Fe _{tot} $\mu\text{g l}^{-1}$	Mn $\mu\text{g l}^{-1}$	Sr $\mu\text{g l}^{-1}$	PO ₄ -P $\mu\text{g l}^{-1}$
<i>Dipwell D4</i>															
0.1	739	93.5	11.75	41.1	7.6	277.3	73.9	27.2	3.22	<0.003	2.46	38	19.1	654	106
0.3	581	67.1	7.81	44.1	2.7	258.2	37.4	17.0	3.68	0.034	2.16	6	1.3	445	92
0.5	490	48.7	7.17	54.8	1.7	195.9	39.7	17.7	1.43	0.033	2.76	3	1.1	343	69
0.7	619	55.8	8.4	61.6	1.4	224.1	62.4	21.0	0.886	0.032	2.37	2	1.0	400	59
0.9	762	71.2	17.44	46.0	1.5	137.3	184.0	12.9	1.20	0.047	2.65	3	2.5	547	93
1.5	715	59.7	19.44	52.3	2.3	163.6	137.6	16.4	0.804	0.044	2.86	<2	1.2	435	83
1.7	687	61.2	18.36	47.6	2.6	161.3	150.1	14.5	0.914	0.044	2.51	2	1.0	470	69
1.9	709	70.7	15.84	52.3	2.5	160.5	141.0	16.0	0.867	0.045	2.27	<2	1.4	489	87
2.1	639	65.6	15.01	34.2	2.3	147.9	116.4	15.4	0.579	0.044	3.08	<2	0.7	519	73
2.5	531	55	13.89	26.3	2.0	170.9	72.2	13.4	0.563	0.042	2.55	<2	0.3	457	66
2.7	483	47.3	12.27	33.6	2.2	162	64.0	15.3	0.831	0.044	2.79	3	0.9	335	93
2.9	531	53.9	13.52	36.8	2.3	170.5	76.6	13.4	0.654	0.043	2.27	3	0.4	427	82
3.1	524	54.8	12.87	30.2	1.8	148.7	80.4	14.7	0.621	0.043	3.45	<2	0.3	417	62
3.5	434	45.6	12.32	27.0	2.0	199.2	32.5	14.6	0.519	0.043	2.61	<2	0.5	324	69
3.7	412	41.7	12.85	26.7	2.4	188.6	31.0	16.5	0.907	0.045	2.82	2	0.6	288	98
3.9	458	44.9	14.25	33.5	3.1	195.2	38.5	17.5	1.87	0.044	2.80	4	0.4	307	75
4.1	513	41.2	17.18	39.5	4.0	215.5	42.9	20.6	1.85	0.046	3.91	2	1.0	293	69
4.5	518	45.7	15.74	39.5	3.4	203.4	48.1	22.5	1.62	0.045	2.68	<2	0.6	316	76
4.7	544	41.8	18.31	44.0	4.1	196.4	54.0	24.0	2.25	<0.003	1.94	7	1.1	290	83
4.9	604	47.6	19.86	48.7	4.8	203.1	60.7	31.8	3.06	<0.003	2.76	4	1.4	335	80
5.1	579	47.2	20	43.4	4.0	177.4	62.1	31.0	5.32	<0.003	2.87	3	0.8	328	80
5.25	562	43.9	16.31	42.9	3.9	157.1	63.9	29.5	5.22	<0.003	4.38	3	1.3	293	88
5.7	493	41	15.97	37.1	3.3	176.9	50.0	20.2	2.30	<0.003	3.05	3	1.1	283	82
5.9	474	42.2	13.91	37.9	2.7	192.4	48.7	14.6	0.882	<0.003	3.02	<2	<0.2	317	59
6.1	518	46.6	12.76	44.7	2.7	210.2	49.4	11.9	0.245	<0.003	3.00	<2	<0.2	361	59
6.5	439	37.6	11.1	39.8	2.40	157.6	41.3	22.0	1.71	0.044	13.8	<4	<0.4	312	117
Mean	594	55.0	15.08	45.1	3.35	188.4	79.49	23.57	1.873	0.0315	2.77	4.35	2.1	408.2	80
Min	412	37.6	7.17	26.3	1.43	137.3	30.99	11.95	0.245	<0.006	1.94	<2	<2	282.9	<50
Max	936	93.5	24.41	82.5	10.5	277.3	218.8	88.4	5.321	0.0517	4.38	38	19.1	653.5	117

Table 3. Major, selected minor and trace element chemistry and stable isotope composition of groundwaters from the Braunton dune system.

Site ID	Date	Temp (°C)	pH	Eh (mV)	DO mg l ⁻¹	SEC µS cm ⁻¹	Ca mg l ⁻¹	Mg mg l ⁻¹	Na mg l ⁻¹	K mg l ⁻¹	HCO ₃ mg l ⁻¹	Cl mg l ⁻¹	SO ₄ mg l ⁻¹	NO ₃ -N mg l ⁻¹	NO ₂ -N mg l ⁻¹	Si mg l ⁻¹	Fe _{tot} µg l ⁻¹	Mn µg l ⁻¹	Sr µg l ⁻¹	P µg l ⁻¹	δ ¹⁸ O ‰	δ ² H ‰	δ ¹³ C _{DIC} ‰
<i>Dune slack</i>																							
1	25-Feb-10	7.9	7.30	139	0.4	719	101.2	14.6	24.8	1.9	373	41.3	8.08	0.01	<0.006	5.23	928.2	972.6	1566	<30	nd	nd	nd
2	25-Feb-10	8.9	7.53	133	0.2	597	81.5	11.1	28.3	1.1	291	42.3	5.17	0.01	<0.006	3.29	613.2	244.8	725	<30	nd	nd	nd
3	25-Feb-10	8.3	7.67	248	0.2	835	68.3	22.0	68.0	3.8	307	94.5	20.47	<.01	<0.006	2.51	11.3	4.2	959	<30	nd	nd	nd
PR2	15-Nov-12	12.2	7.57	148	0.5	599	58.6	22.5	77.8	3.9	306	120.5	38.58	2.43	<0.006	3.94	106.4	163.0	nd	<30	-5.40	-34.9	-8.9
<i>High dune</i>																							
D4	15-Feb-12	10.4	7.93	-190	1.1	804	65.1	26.8	54.2	4.0	285	111.3	21.16	0.95	<0.003	3.66	231	470	779	<10	-5.90	-38.4	-9.5
D5	15-Feb-12	12.1	7.98	-318	0.5	687	62.6	23.0	43.7	2.8	330	73.2	15.99	0.01	<0.003	3.75	303	566	1230	<10	-5.97	-40.6	-9.3
<i>Pilton Mudstone formation</i>																							
Golf Club	14-Nov-12	12.0	7.20	231	0.9	877	72.4	16.7	28.4	1.5	254	43.02	7.15	0.02	<0.003	4.35	94.4	136.6	nd	<10	-5.82	-35.9	-13.6

Table 4. SF₆ concentrations as measured and also corrected for excess air inputs (see text), with calculated mean residence times (MRTs) for groundwater below dune slacks and high dunes.

Dipwell	Site type	Date	SF₆ (fmol/L)	SF₆ corr. (fmol/L)	MRT (yr)
D1	Dune slack	25-Feb-10	2.65	2.29	6 ± 2
D2	Dune slack	25-Feb-10	2.49	2.15	7 ± 2
D3	Dune slack	25-Feb-10	2.73	2.36	6 ± 2
Dnew4	High dune	15-Feb-12	1.76	1.52	16 ± 2
Dnew5	High dune	15-Feb-12	2.06	1.78	13 ± 2
Golf Club	Bedrock	14-Nov-12	1.31	1.04	22 ± 2.5